CMLS, Cell. Mol. Life Sci. 61 (2004) 1198–1207
1420-682X/04/101198-10
DOI 10.1007/s00018-004-4045-8

CMLS Cellular and Molecular Life Sciences

Research Article

Profile identification of disease-associated humoral antigens using AMIDA, a novel proteomics-based technology

O. Gires[a, b, *], M. Münz[b], M. Schaffrik[b], C. Kieu[a], J. Rauch[a], M. Ahlemann[a], D. Eberle[a], B. Mack[a], B. Wollenberg[a, b], S. Lang[a], T. Hofmann[a], W. Hammerschmidt[c] and R. Zeidler[d]

[a] Department of Head and Neck Surgery, Ludwig-Maximilians University of Munich, Marchioninistr. 15, 81377 Munich (Germany), Fax +49 89 70956896, e-mail: ogires@hno.med.uni-muenchen.de
[b] Clinical Cooperation Group Molecular Oncology Department of Head and Neck Research, Ludwig-Maximilians University, Marchioninistr. 15, 81377 Munich (Germany)
[c] GSF-National Research Center for Environment and Health, Department of Gene Vectors, Marchioninistr. 25, 81377 Munich (Germany)
[d] Vaecgene Biotech Inc., Marchioninistr. 25, 81377 Munich (Germany)

Received 30 January 2004; received after revision 3 March 2004; accepted 8 March 2004

Abstract. We describe AMIDA (autoantibody-mediated identification of antigens), a novel target identification technology based on the immunoprecipitation of disease-specific antigens by autologous serum antibodies followed by two-dimensional electrophoretic separation, and their identification via mass spectrometry. Twenty-seven potential carcinoma antigens were identified including proteins of hitherto unknown function. Validation of one of the identified antigens, cytokeratin 8, revealed its de novo expression in hyperplastic tissue, gradual overexpression with increasing malignancy, and ectopic localization on the cell surface. Furthermore, a strong prevalence of CK8-specific antibodies occurred in the serum of cancer patients already at early disease stages. In situ hybridization for one marker of unknown function, KIAA1273/TOB3, demonstrated its strong overexpression in head and neck carcinomas, thus making it a likely tumor antigen candidate. Eventually, AMIDA could foster significant improvements for the diagnosis and therapy of human diseases eliciting a humoral immune response, and allows for the rapid identification of new target molecules.

Key words. AMIDA, CK8, KIAA1273/TOB3, humoral antigens, HNSCC.

Molecular diagnostics for the early detection of tumors have become a challenging priority due to the high mortality caused by cancer. Accordingly, proteomic approaches have experienced a strong revival and are of acknowleged importance with respect to target protein identification [1]. Targets, i.e., disease-specific markers, are of use for antibody-based approaches, DNA or protein vaccination, and the generation of antigen-specific cytotoxic T lymphocytes. In vivo, the humoral response is one of the weapons of our immune system to fight pathogens and transformed cells. Therefore, sera from individuals encountering infectious pathogens or developing malignancies contain disease-specific antibodies directed against antigenic epitopes. Given the presence of such antibodies in patients, we have established a novel proteomics-based technology allowing for the isolation and identification of the cognate antigens. We named this technology AMIDA, for autoantibody-mediated identi-

* Corresponding author.
O. Gires, M. Munz and M. Schaffrik contributed equally to this work.

fication of antigens. Considering posttranscriptional and -translational modifications, an estimated 300,000–500,000 proteins are likely expressed by the human genome. AMIDA uses the hosts' humoral responses as a biological filter to focus on and isolate potential targets among this vast number of proteins. AMIDA was applied in an autologous fashion, that is, covalently matrix-bound serum antibodies from patients were used to immunoprecipitate potential disease-specific proteins from lysates of the autologous malignant tissue. The retrieved proteins were separated by two-dimensional gel electrophoresis (2DE) and analyzed by matrix-assisted laser desorption ionization-time of flight mass spectrometry (MALDI-TOF). In the present study, we concentrated on the identification of potential carcinoma-associated targets. AMIDA was applied to six cases of carcinomas of the upper aerodigestive tract. A total of 27 proteins were identified, 11 of which have already been described as tumor- or autoimmune disease-associated molecules. The remaining 16 proteins are new potential tumor-associated antigens, the function of 7 of these proteins has not yet been assigned.

In the following, cytokeratin 8 (CK8), which was isolated from a membrane fraction of tumor cells, suggesting its aberrant expression in carcinomas of the upper aerodigestive tract, was analyzed in more detail. CK8 was detected early in hyperplasia, strongly overexpressed in carcinomas, and at the plasma membrane of primary carcinomas and tumor cell lines. Additionally, we demonstrated elevated titers of CK8-specific serum antibodies in carcinoma patients at early stages of disease, making it a potential diagnostic tumor marker. In addition, the mRNA expression of one protein of still unknown function, the AAA-ATPase TOB3, was assessed by *in situ* hybridization in healthy mucosa and primary head and neck carcinomas. TOB3 was strongly overexpressed in primary carcinomas with a homogenous distribution within the tumor mass. Thus, AMIDA is a novel and rapid technology dedicated to the enrichment and separation of proteins specific for a given disease, which are targets of the humoral response.

Material and methods

Cell lines, primary tumor cells, flow cytometry, and immunofluorescence

GHD-1 cells were established in our laboratory from a biopsy of a hypopharynx carcinoma patient enrolled in the AMIDA screening. PCI-1/13, HLAC78/79, ANT-1, FaDu, and 22A are carcinoma cell lines of the upper aerodigestive tract. SkBr3 and MCF-7 are breast, Hela is a cervix, and HCT-8 a colon carcinoma cell line. HEK293 are epithelial human embryonical kidney cells immortalized by adenoviral E1A and E1B. All cell lines were cultured in standard DMEM supplemented with 10% (v/v) fetal calf serum (FCS). Primary carcinoma biopsies were minced and incubated in DMEM containing collagenase (2 mg/ml, type 8; Sigma, Taufkirchen, Germany) and DNAse I (0.2 mg/ml, type IV, Sigma) for 2 h at 37 °C. Cells were washed twice in PBS and resuspended in PBS supplemented with 3% (v/v) FCS for immuno- and flow cytometry staining. Non-permeabilized cells (5×10^5) were incubated with CK8-specific 1E8 antibody (Hess Diagnostics, Freiburg, Germany) for 1 h at 4 °C, washed in PBS with 3% FCS, and stained with a FITC-labeled secondary antibody (30 min, 4 °C), and analyzed in a FACScalibur device (Becton Dickinson, Heidelberg, Germany). Alternatively, cells were fixed (1% PFA, 10 min) and permeabilized (0.2% Triton, 20 min) before staining. For immunofluorescence, cells were cytospun on glass slides, stained for CK8 and EpCAM with specific monoclonal antibodies (1E8 and C215, respectively) and PE- and FITC-conjugated secondary antibodies.

Immunoprecipitation, 2DE and mass spectrometry

For membrane fractionation, primary carcinoma cells or GHD-1 cells (1×10^7) were obtained as described above, washed once in PBS and incubated in hypotonic buffer containing 10 mM HEPES (pH 7.9), 10 mM KCl, 1.5 mM MgCl, 0.1 mM EGTA and 0.5 mM DTT for 30 min. Cells were dounced with a 23G-needle, the particulate fraction centrifuged (3000 g; 4 °C), and proteins solubilized in 50 mM tris-buffered saline (TBS) with 1% (v/v) Triton X-100. Alternatively, whole cell lysates were generated from 2.5×10^7 cells in TBS containing 1% (v/v) Triton X-100. Lysates were precleared with sepharose A beads (Amersham Biosciences Europe, Freiburg, Germany) for 3 h at room temperature in a tumbler. Immunoprecipitation was performed in an autologous fashion with sepharose A beads precoated with patient serum (300 µl serum, 50 µl beads, overnight, 4 °C, tumbler). Immunoglobulins were covalently cross-linked to the sepharose matrix following the protocol described by Schneider et al. [2]. After immunoprecipitation, beads were washed extensively in 50 mM TBS, resuspended in 2D lysis buffer (9 M urea, 4% CHAPS, 65 mM DTT, 5 mM EDTA) and centrifuged (42,000 g, 1 h, 4 °C). Proteins in the supernatant were separated by isoelectric focussing using immobilized pH gradients pH 3–10 or 4–7 (IPG strips; Amersham) at 60 kVh and, according to their molecular weight, in 12% SDS-PAGE. Proteins were visualized by Coomassie or silver staining, immunoprecipitated protein spots isolated, digested with trypsin (2.5 ng/µl; Promega, Mannheim, Germany) and analyzed in a MALDI-TOF mass spectrometer (Reflex III; Bruker, Leipzig, Germany). Protein identification was performed with the resulting peptide mass fingerprints using Matrix Science (www.matrixscience.com). Standard search parameters were used – taxonomy: homo sapiens, enzyme:

trypsin, fixed modifications: carbamidomethyl, variable modifications: oxidation (M), peptide tolerance: 150 ppm.

Quantification of antibody titers

Recombinant human CK8 protein (5 µg; Progen, Heidelberg, Germany) was coated on fluorescence-labeled beads (100 µl = 1.25×10^6 beads) with the Bioplex amine coupling kit (Bio-Rad, Munich Germany). Serum from healthy volunteers and carcinoma patients (1:100 dilution) was tested for CK8-specific antibodies by incubation with CK8-coated beads (1 µl, 1 h, room temperature) and subsequent detection using PE-coupled antibodies specific for human IgGs (30 min, room temperature). The measurement of bead and PE fluorescence was performed in a Bioplex system. PE fluorescences of the individual samples were compared for 100 labeled beads of each sample and expressed as mean fluorescence intensities (MFI). Significance was calculated with an unpaired students t test. Sensitivity (s) was determined as follows: s = a:(a+b) where a is the number of tumor sera above the cutpoint and b below the cutpoint. Specificity is the percentage of healthy donor sera below the cutpoint. The cutpoint was set to 4000 MFI. Unspecific binding of serum antibodies was tested with bovine serum albumin-coated beads.

Immunohistochemistry

Specimens of squamous cell carcinoma were obtained from 25 patients undergoing surgery. Healthy mucosa were used as negative controls and were obtained during routine biopsy by surgery. Briefly, tissue was shock frozen in liquid nitrogen and cut into 5 µm-thick sections. For immunohistological staining, monoclonal mouse anti-human cytokeratin 8 antibody clone 35βH11 (DAKO, Glastrup, Denmark) was used. The antigen-antibody reaction was detected using the avidin-biotin-PO (ABC) method as described before [3]. Analysis of staining intensities was performed by two experienced investigators independently.

In situ hybridization

Frozen tissue sections (5 µm) were fixed in 4% paraformaldehyde and washed in PBS, dehydrated in graded ethanol and stored at –70 °C. After thawing, inactivation of endogenous alkaline phosphatase with HCl (0.2 N), and digestion with Proteinase K (10 µg/ml), the slides were treated with 0.1 M glycine/0.05 M PBS and 4% paraformaldehyde at room temperature. Washing steps with PBS were carried out between every treatment. Then, sections were permeabilized with 0.1 M triethanolamine/0.25% acetic anhydride, washed with 2×SSC and incubated in prehybridization buffer (5 h, room temperature, 50% deionized formamide, 4× SSC, 5× Denhardt's, 25 µg/ml salmon sperm DNA, 0.1% SDS, 50 µg/ml t-RNA, 5% dextran sulfate). KIAA1273/TOB3 cDNA was amplified by PCR using the forward primer 5′-CGATGGTACCGA TCCTGGGTGCAGATGCAGC-TGGAAG-3′ and the backward primer 5′-ATCGCT-CGAGCTACAACAGGGGGTGCCCTGGGGG-3′ with the RZPD clone IRALp962O1117 as a template. The PCR product was cloned into the pDrive vector (Qiagen, Hilden, Germany). pDrive-KIAA1273/TOB3 was linearized by *Bam*HI or alternatively *Hind* III digestion for in vitro transcription to produce sense and antisense DIG-labeled RNA probes using the DIG RNA Labeling kit (Roche, Mannheim, Germany) including T7 and SP6 RNA polymerases. Resulting probes were diluted in prehybridization buffer for hybridization of sections overnight at 70 °C. After stringent washing (2 × SSC and 0.2 × SSC), sections were further washed with T1 buffer (0.5 M maleic acid, 750 mM NaCl, pH 7.5), and incubated in T2 buffer (T1 buffer + 1% blocking reagent, 1 h, room temperature). Thereafter, sections were incubated (1 h, room temperature) with an alkaline phosphatase-conjugated anti-DIG antibody (Roche). Signals were visualized with nitroblue tetrazolium (NBT) and 5-bromo-4-chloro-3-indolyl phosphate (BCIP) as substrates (Roche). The reaction was stopped by washing slides in PBS buffer. For each test, control experiments using DIG-labeled sense RNA probes were performed in parallel.

Results

Identification of tumor-associated antigens using AMIDA

Sera from patients suffering from squamous cell carcinomas of the upper aerodigestive tract were collected together with specimens of the autologous tumors and subjected to an AMIDA screen as schematically depicted in figure 1. Cancer cell biopsies were processed to single-cell suspensions and a defined cell number was lysed to obtain crude protein preparations or membrane-associated protein fractions. Potential tumor-associated antigens (TAAs) were recovered by overnight immunoprecipitation (IP) with immobilized autologous serum antibodies and separated by 2DE and stained with silver nitrate or Coomassie, as described in Materials and methods. As a control, autologous leukocytes were processed as a protein reference in parallel with tumor material. Serum antibodies coupled to sepharose A beads were processed likewise and served as a second negative control in order to exclude proteins which would represent false positives of the system. Analysis of 2DE protein patterns and the discrimination of differential protein spots were performed with the Image Master 2D software (fig. 1, 2). Tumor-IP-specific protein spots were excised, subjected to an in-gel tryptic digest, and the resulting peptides analyzed by MALDI-TOF MS with an identifica-

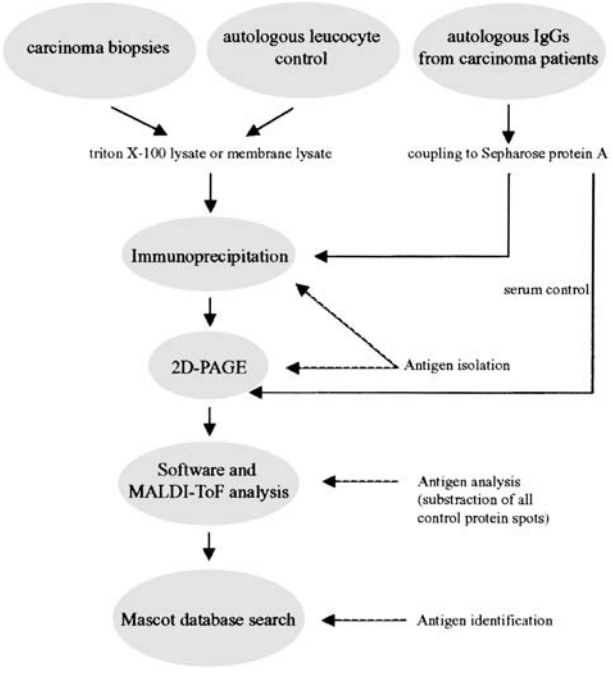

Figure 1. Flow chart of the autologous AMIDA screening technology.

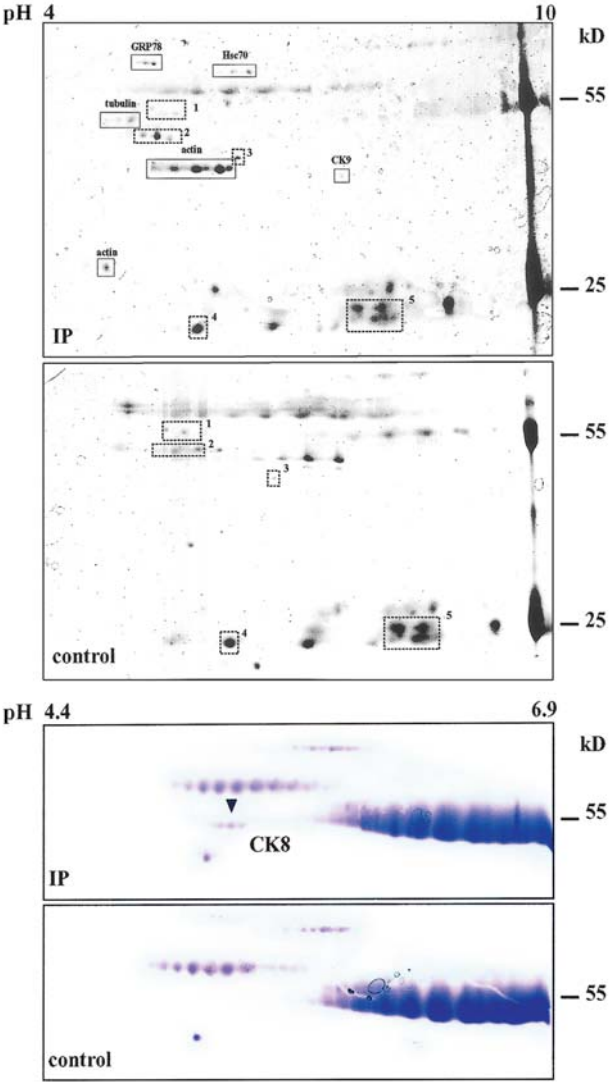

Figure 2. Sections of two-dimensional gels from AMIDA 2DE gels stained with silver nitrate (*a*) or with Coomassie blue (*b*). Spots isolated and identified upon MALDI-TOF MS are indicated. Shown are representative immunoprecipitation and serum control 2DE gels. (*a*) Addtitional spots are marked by dotted quadrants and numbered to serve as landmarks for easier orientation.

tion rate of 50% in average for silver-stained and 80% for Coomassie-stained protein spots. A total of six squamous cell carcinomas of the upper aerodigestive tract were screened independently. After the exclusion of immunoglobulins and soluble serum proteins, a total of 27 potential tumor-associated antigens remained (table 1), representing 70–80% of all proteins identified by MALDi-TOF MS. The 27 proteins identified could be assigned to one of the following three groups. (i) Proteins already defined as TAAs such as grp78 [4], or proteins associated with autoaggressive immunity such as AHNAK nucleoprotein [5], vimentin [6], and hsc70 [7]. (ii) Proteins of known function, which had not been associated with cancer (tropomyosin alpha, elongin A2). (iii) Proteins of unknown function (KIAA proteins, hypothetical 41.3-kDa protein). The accession number, identification score, protein source, reference, matched peptides, and sequence coverage for all proteins identified are listed in table 1. Four proteins, namely keratin 16, ATP synthase beta chain, beta actin and mutant keratin 9, were isolated from two or more patient samples (table 1). One difficulty hampering the multiplication of AMIDA screens from one single patient is the necessity for a minimal number of tumor cells, i.e., 1×10^7 cells per immunoprecipitation. To circumvent this issue and to assess the reproducibility of the AMIDA technology, a cell line, termed GHD-1, was generated from a biopsy of the primary carcinoma of one patient enrolled in the AMIDA screening. This allowed the repeated immunoprecipitation of proteins from the autologous carcinoma cell line with serum antibodies of the patient. The results demonstrated the high reproducibility of the AMIDA screen method: in a total of four independent screenings performed with the GHD-1 cell line, the AMIDA antigen CK8 was isolated four times with mass spectrometry Mowse scores ranging from 336 to 473, all being highly significant. Additional antigens isolated from the primary carcinoma cells originating from the patient's biopsy were also identified in three out of four experiments.

CK8 expression on the carcinoma cell surface

Among the proteins of known function, four different cytokeratins, namely keratin 6d, 8, 9, and 16, were isolated. Of note, CK6d and CK8 have been retrieved from mem-

Table 1. Accession number, protein name and identification scores of the isolated AMIDA antigens.

Acc. N°.	Protein	ID score	Source	Reference	Matched peptides	Seq. cov.	Occur.
Q96I66	unknown protein	72	WCL	TREMBL	7	18%	1/6
JC4313	keratin 16	71	WCL	TAA [21]	9	28%	2/6
Q96PV1	KIAA1937	99	WCL	[22]	13	19%	1/6
P35557	D-glucose hexokinase	75	WCL	TAA [23]	8	7%	1/6
Q9p2V9	elongin A2	66	WCL	[24]	13	13%	1/6
P06753	tropomyosin alpha	72	WCL	[25]	11	48%	1/6
Q9ULK3	KIAA1217	65	MF	[22]	8	9%	1/6
1MABB	ATP synthase beta chain	129	MF	[26]	17	27%	2/6
P08670	vimentin	298	MF	a-Ag [27]	36	64%	1/6
Q96LL7	CDNA FLJ25393	64	MF	TREMBL	9	14%	1/6
P11021	Grp78	269	WCL	TAA [4]	24	47%	1/6
1KAX	heat shock cognate protein 70	99	WCL	a-Ag [7]	29	46%	1/6
Q91575	tubulin beta	240	WCL	TAA [28]	25	51%	1/6
ATHUB	actin beta	146	WCL	TAA [28]	18	50%	3/6
ATHUG	actin gamma	161	WCL	TAA [28]	19	48%	1/6
D42825	Kruppel-type zink finger protein ZNF-70	76	WCL	[29]	6	38%	1/6
CSHUA	cyclophilin A	66	WCL	TAA [30]	6	41%	1/6
O00109	mutant keratin 9	110	WCL	[31]	13	28%	3/6
BAA86587	KIAA1273/TOB3	100	MF	[22]	6	19%	1/6
P05787	keratin 8	473	MF	TAA [8, 9]	36	56%	1/6
S55024	nebulin	87	MF	[32]	35	15%	1/6
I61769	keratin 6d	129	MF	TAA	18	55%	1/6
Q9Y2K3	KIAA1000	63	WCL	[22]	17	23%	1/6
Q96ES1	similar to serine proteinase	107	WCL	[33]	11	35%	1/6
C1HURB	complement subcomponent C1r	134	WCL	[34]	14	39%	1/6
Q9B5S71	hyp. 41.3 kDa protein	97	WCL	TREMBL	9	32%	1/6
Q9UJD9	similar to RPS2	69	WCL	TREMBL	12	41%	1/6

ID, identification. A score ≥62 represents a p value <0.05. WCL, whole-cell lysate; MF, membrane fraction; a-Ag, autoantigen; TAA, tumor-associated antigen, TREMBL data base entry. Seq. cov., sequence coverage upon MALDI-TOF analysis; Occur., occurrence in patients.

brane fractions with autoantibodies, suggesting an aberrant localization of these normally cytoplasmic proteins. This ectopic expression is one possible explanation for the induction of specific antibodies against these proteins. Thus, we analyzed the expression of CK8 on the surface of the cell line GHD-1, which was established from the primary carcinoma of the patient from whom CK8 was isolated. Non-permeabilized GHD-1 cells were stained with the CK8-specific antibody 1E8, which has already been reported to recognize a CK8 epitope on the surface of breast carcinoma cells [8, 9]. Cell surface expression of CK8 was analyzed by flow cytometry and was detectable on the surface of vital, non-permeabilized GHD-1 cells. The amount of membrane-associated CK8 was lower compared to the levels of cytoplasmic CK8 (fig. 3a). We also observed staining of non-permeabilized carcinoma cell lines using two different pan-CK antibodies (fig. 3a and data not shown), an indication for the presence of additional cytokeratins at the cell surface, in line with previous findings [10] and our own results (table 1). The staining pattern of CK8 in head and neck carcinoma cells was additionally determined by immunofluorescence: cytospins of non-permeabilized FaDu cells were co-stained with CK8- and EpCAM-specific anti-

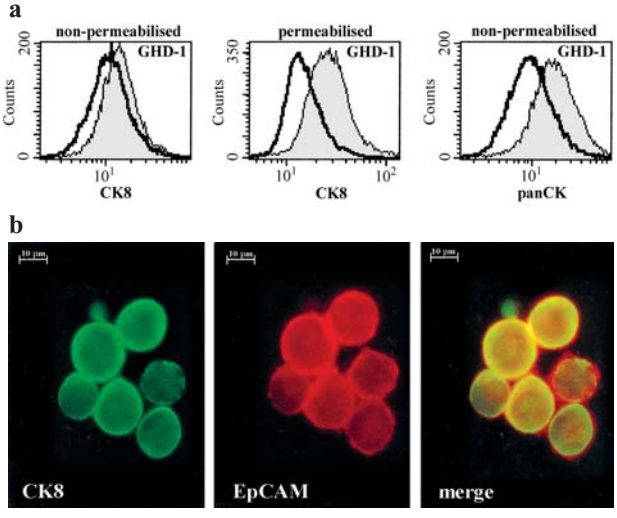

Figure 3. FACS analysis of CK8 expression on carcinoma cell lines. (*a*) GHD-1 tumor cells were either untreated or permeabilized and stained with the CK8-specific monoclonal antibody 1E8 in combination with a FITC-labeled secondary antibody. In addition, non-permeabilized GHD-1 cells were incubated with a pan-CK antibody (CK2, 5, 6, 8, 10, 11, 14/15, 18, 19). (*b*) Cytospins of FaDu cells (4×10^5) were stained with the CK8-specific 1E8 antibody in combination with a FITC-conjugated secondary antibody (left), and with the EpCAM-specific antibody C215 in combination with a Cy3-conjugated secondary antibody (middle) in double stainings.

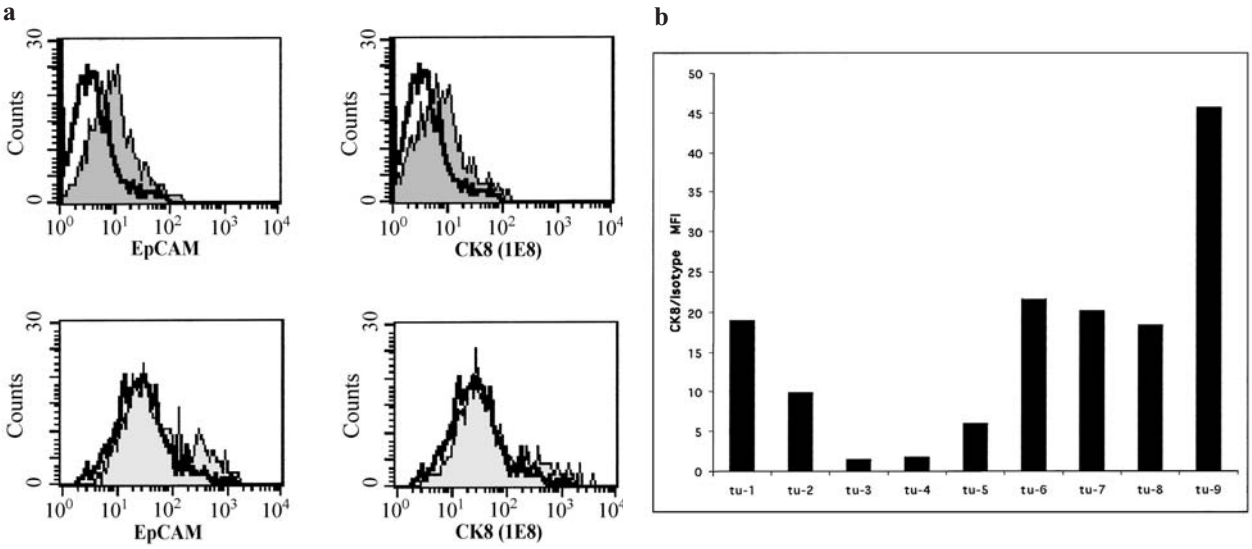

Figure 4. FACS analysis of CK8 expression on primary carcinoma cells. (*a*) Single-cell suspensions of HNSCC biopsies were generated and stained with CK8- and EpCAM-specific antibodies in combination with a FITC- and PE-conjugated secondary antibody, respectively. PI-negative cells and EpCAM-positive carcinoma cells expressed CK8 on the cell surface (upper histograms). Large EpCAM-negative tumor-infiltrating cells were negative for CK8 (lower panel). (*b*) Shown are the mean CK8 fluorescence stainings of nine cell suspensions generated from primary tumors corrected for the mean fluorescence of the corresponding control (CK8/isotype MFI).

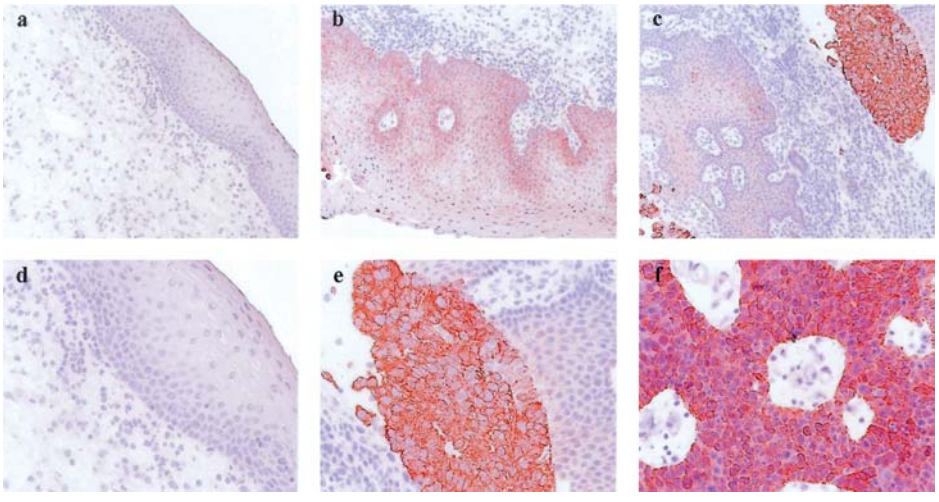

Figure 5. CK8 expression in healthy mucosa, hyperplasia and carcinomas. Crysections of tumor biopsies were stained with the CK8-specific antibody 1E8 in combination with a conjugated secondary antibody. Sections of one patient showed areas of intact, healthy mucosa (*a*, *d*), hyperplastic tissue (*b*, *c*) and tumor (*c*, upper right part and *e*) which stained differentially for CK8. The CK8 staining of one head-and-neck carcinoma metastasis is shown in *f*.

bodies. The epithelial cell adhesion molecule EpCAM is an integral membrane protein overexpressed in carcinoma cells [11]. Immunofluorescence demonstrated that both proteins are located at the plasma membrane and show overlapping staining patterns as demonstrated in merged images (fig. 3b).

To further validate our findings, we assessed the surface expression of CK8 on primary carcinomas of the aerodigestive tract. Single-cell suspensions were generated from nine freshly isolated primary tumor biopsies and stained with the CK8-specific antibody 1E8. The pan-carcinoma antigen EpCAM served as a marker for carcinoma cells and propidium iodide (PI) exclusion was performed to define vital cells. Figure 4a shows the flow cytometry analysis of tumor number 4, which expressed CK8 on the surface of EpCAM-positive intact carcinoma cells. Of note, large tumor-infiltrating cells, as defined by the negative staining for EpCAM and the specific morphology, did not stain for CK8 (fig. 4a, lower panel). The analysis of nine carcinoma biopsies demonstrated that

CK8 was expressed strongly on the tumor cell surface in six out of nine cases. One tumor showed moderate expression, while two tumors expressed low amounts of CK8 on the cell surface, including tumor 4 (fig. 4b). Thus, CK8 was ectopically expressed on the cell surface of all primary tumors studied and was absent from tumor-infiltrating cells.

For information on the expression profile of CK8 in vivo, we performed immunohistochemistry on cryosections of tumor biopsies. Intact, healthy epithelium did not express CK8 (fig. 5a, d), whilst hyperplastic epithelium of the same patient displayed detectable CK8 staining, which was most prominent in areas of cellular outgrowth (fig. 5b, c). Tumor areas of the patient's biopsy stained strongly postive, demonstrating the gradual overexpression of CK8 (fig. 5e). Furthermore, tumor metastasis showed intense CK8 staining, which was strictly restricted to the tumor cell mass (fig. 5f).

Quantification of CK8-specific antibodies in serum

The presence of CK8-specific antibodies in one cancer patient, which allowed the isolation of CK8, prompted us to assess the frequency and titer of antibodies to CK8 in other patients and also in healthy volunteers. For this, we used an adapted Bioplex system [12], which combines the principle of an ELISA with the Luminex fluorescent bead-based technology. Recombinant human full-length CK8 was covalently bound to beads and incubated with serum from healthy volunteers (n=67) or carcinoma patients (n=60) in combination with a PE-conjugated human IgG-specific antibody. The relative PE fluorescence was determined in a Bioplex system. Limited CK8 reactivity was observed in healthy donors (overall mean: 2500 MFI), whereas the frequency and titer of CK8-specific antibodies was significantly higher in carcinoma patients (overall mean: 9500 MFI, $p \leq 0.0001$) (fig. 6a). Interestingly, the highest CK8-specific antibody titers were detectable in patients with early stage disease (T1/2). More advanced stages were characterized by somewhat weaker humoral responses (fig. 6b), possibly due to immunosuppressive effects of tumor cells. A cut-off point was set according to the primary data to calculate the specificity and sensitivity of CK8 antibodies in patient blood as a tumor marker. The calculated overall sensitivity including all TNM stages was 83.3% and specificity was 89.5%. With TNM1-staged patients, the sensitivity was even higher (88.9%) while specificity remained unchanged (89.5%) Additionally, a total of 21 patients were analyzed for a potential correlation of the expression level of CK8 and the titers of anti-CK8 autoantibodies in the serum. A tendency towards a diminished antibody titer in patients with high CK8 levels was observed. However, the differences were only slight and not significant (data not shown).

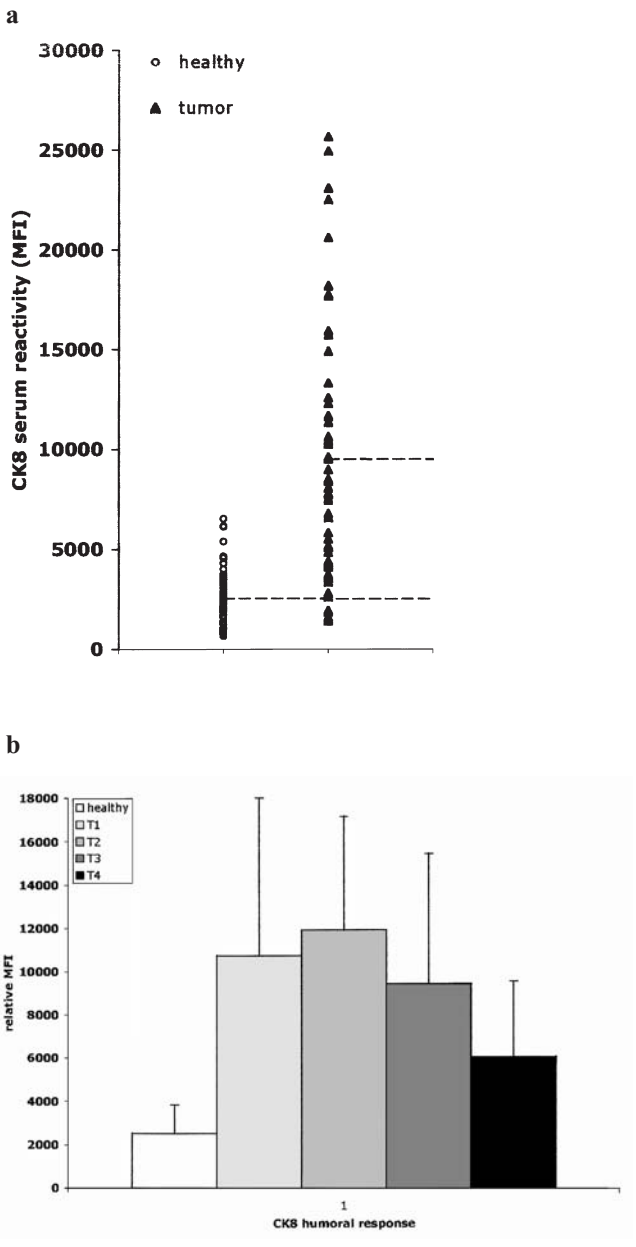

Figure 6. Recombinant human CK8 was coupled to fluorescence-labeled beads and incubated with healthy donor or carcinoma patient sera (1:100 dilution). Afterwards, the bound antibodies were stained with a PE-conjugated secondary antibody against human immunoglobulins. Bead and PE fluorescence were measured in a Bioplex device (BioRad). (*a*) MFI from independent duplicated data sets. Open circles represent healthy donors, closed triangles represent carcinoma patients (p value <0.0001). Mean MFI values are indicated by a dashed line for both conditions. (*b*) Mean values of MFI, including standard deviations from healthy donor and carcinoma sera. The CK8 humoral response was correlated to the TNM status of patients, and shown as MFI with standard deviations from two independent experiments. p values: healthy/T1 = 0.006; healthy/T2, T3, T4 < 0.0001.

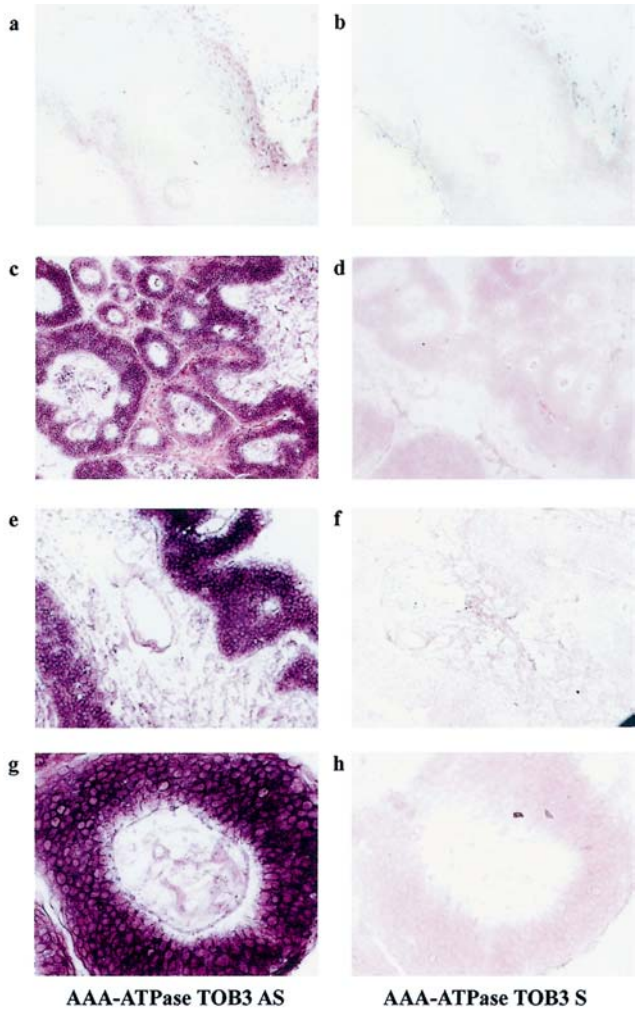

Figure 7. TOB3 mRNA expression in healthy mucosa and carcinomas. Cryosections of healthy mucosa (*a*, *b*) and carcinoma specimens (*c*–*h*) were analyzed by in situ hybridization using a labeled KIAA1273/AAA-ATPase TOB3 complementary antisense RNA (AAA-ATPase TOB3 AS) and as a control, a labeled KIAA1273/AAA-ATPase TOB3 sense RNA (AAA-ATPase TOB3 S). Healthy mucosa stained weakly with the complementary RNA in cells of the basal membrane layer, while carcinoma cells showed a strong and specific staining.

TOB3 is specifically expressed in carcinoma cells

The AMIDA screenings resulted in the isolation and identification of seven proteins of unknown function (see table 1), which may represent entirely new TAAs. The mRNA expression of one of these proteins, KIAA1273, was assessed in cryosections of healthy mucosa and head-and-neck primary carcinoma by in situ hybridization in order to examine its tumor specificity. Recent data base entries showed that KIAA1273 was the novel TOB family member TOB3. Thus, in the following, the TOB3 nomenclature will be used. We observed weak TOB3 mRNA expression in the basal membrane layer of healthy mucosa, while higher differentiated epithelia did not express TOB3 mRNA (fig. 7a). In sharp contrast, carcinoma cells of head-and-neck specimens expressed large amounts of the mRNA for TOB3 (fig. 7c, e, g). Thus, TOB3 was de novo expressed in carcinoma cells of the upper aerodigestive tract.

Discussion

We present here a new combinatorial technology, dedicated to the identification of disease-specific antigens at the protein level in an autologous fashion, termed AMIDA. Here, AMIDA was applied to carcinoma samples in order to identify TAAs which can be used as diagnostic and/or therapeutic targets. A substancial number of the 27 proteins retrieved from six carcinoma patients are known TAAs or are involved in autoimmune diseases (table 1). The isolation of 11 proteins already described in association with cancer or autoimmune diseases clearly confirmed the potential of AMIDA to identify disease-associated proteins with high sensitivity and efficacy. Furthermore, the reproducibility of the technology was very high, as assessed upon repeated screening of the autologous tumor cell line of one patient with the cognate serum antibodies. In the present study, we concentrated further on CK8 as a TAA, its aberrant localization and the presence of CK8-specific antibodies in cancer patients. As shown in figure 2, CK8 was immunoprecipitated as three distinct proteins with comparable molecular weight but differing isoelectric points. Similar results concerning the expression of posttranslationally modified variants of CK8 were reported in the case of lung adenocarcinomas [13]. Interestingly, two of the CK8 variants isolated upon AMIDA screenings had migration properties similar to variants overexpressed in lung adenocarcinomas, as reported by Gharib et al. [13]. Detailed studies showed that CK8 was present on the cell surface of all primary squamous cell carcinomas tested and on the great majority of carcinoma cell lines of different localization (figs. 3, 4 and data not shown). This is in accordance with findings by Hembrough et al. [8, 9], who demonstrated the cell surface expression of CK8 on breast carcinoma cells. Its aberrant localization makes CK8 a potential candidate for antibody-based therapy designed to redirect immune cells to tumor cells, or to eliminate tumor cells using toxin-coupled or radiolabeled monoclonal antibodies. The potential of high-affinity radiolabeled CK8-specific antibodies for in vivo diagnosis and therapy is under current investigation in our laboratory using a tumor mouse model. The finding of a strong immunoreactivity against CK8 in cancer patients as compared to healthy donors (fig. 6) confirmed the rationale of the AMIDA technology, namely the presence of tumor-specific antibodies in patient serum. Additionally, these findings demonstrate that serum antibodies are versatile and sensitive tools for

the identification of tumor antigens. Even more important, CK8-specific antibodies are highly specific and sensitive serological tumor markers for the head-and-neck squamous cell carcinoma early diagnosis that are already present in the serum of patients with early disease stages (fig. 6b). The de novo expression of CK8 in hyperplastic premalignancies, as shown in figure 5b, c, and also the occurrence of soluble CK8 protein in patient serum as has been shown in the case of lung adenocarcinoma [14], may represent one of the determinants for the mounting of a humoral response against CK8 at early stage disease. However, a single parameter will be of limited clinical value. Rather, simultaneous assessement of a panel of reliable markers seems promising. Nevertheless, CK8-specific antibodies possess high sensitivity and specificity compared to parameters routinely used for cancer early detection such as the prostate-specific antigen PSA [15].

The high recovery of hitherto unknown TAA s-16 out of 27 isolated proteins – further underscored the potential of AMIDA and also prompted us to characterize these antigens in more detail. We concentrated initially on one target termed KIAA1273 at the time of identification. Recently, KIAA1273 was renamed the AAA-ATPase TOB3 based on complete sequence homology. TOB3 is a newly identified member of the TIS21/PC3/BTG1/TOB family, which contains a putative AAA-ATPase motif, with unknown function [C. Parng, P. A. Piepenhagen, J. Casanova and S. Pillai unpublished data; http://harvester.embl.de/harvester/Q96T/Q96T67.htm]. Our initial characterization of TOB3 demonstrated its specific de novo expression in carcinoma cells, making it a worth TAA candidate (fig. 7). Also of interest, TOB3 was described recently as a direct target gene of the oncogene c-myc [16]. The oncogenic transcription factor c-myc is involved in processes of cell cycle regulation, metabolism and apoptosis [17] and is upregulated in a great variety of malignancies [18] including head and neck carcinomas [19]. Thus, one is tempted to speculate that TOB3 overexpression results from the direct influence of c-myc activity in cancer cells, although this clearly remains to be proven. Studies aiming at the elucidation of TOB3 expression, function, and regulation in epithelial cells are ongoing in our laboratory.

In conclusion, we provide here a powerful new technology for the identification of tumor markers, proteins involved in autoimmunity or infectious diseases, in an autologous setting. Compared to other technologies AMIDA has a number of advantages. (i) Target identification is performed with the authentic tumor sample, which allows the detection of posttranscriptional and -translational modifications specific to tumor cells, including glycosylation occurring specifically in tumor cells [20] and other modifications. (ii) AMIDA does not necessitate the laborious generation of a cDNA library derived from diseased tissue, nor does it require a heterologous expression system such as bacteria or eukaryotic cells. (iii) AMIDA makes use of immunoprecipitation as a filter to massively reduce the complexity of the protein mixture and to select for proteins of immunological importance to be separated by 2DE and screened. This is of note, taking into account that current protocols of 2DE allow for the high-resolution separation of approximately 1500–3000 proteins per gel, which may at best represent 10–15% of the proteome. (iv) AMIDA can be semi-automated based on the use of 2DE gels as a mode of protein separation and mass spectrometry for the identification of these proteins. These features of AMIDA will allow screening of a large number of patients in a reasonably short period of time to generate specific cancer antigen profiles for different tumor entities or even infectious agents. Such antigen and antibody profiles should not only improve serum-based diagnostics directed toward cancer, but allow for the identification of therapeutically relevant targets.

Acknowledgement. Part of this work was funded by the Else Kröner-Fresenius. We thank E. Kremmer for support with monoclonal antibodies.

1 Hanash S. (2003) Disease proteomics. Nature **422:** 226–232
2 Schneider C., Newman R. A., Sutherland D. R., Asser U. and Greaves M. F. (1982) A one-step purification of membrane proteins using a high efficiency immunomatrix. J. Biol. Chem. **257:** 10766–10769
3 Hsu S. M, Raine L. and Fanger H. (1981) The use of antiavidin antibody and avidin-biotin-peroxidase complex in immunoperoxidase technics. Am. J. Clin. Pathol. **75:** 816–821
4 Mintz P. J., Kim J., Do K. A., Wang X., Zinner R. G., Cristofanilli M. et al. (2003) Fingerprinting the circulating repertoire of antibodies from cancer patients. Nat. Biotechnol. **21:** 57–63
5 Skoldberg F., Ronnblom L., Thornemo M., Lindahl A., Bird P. I., Rorsman F. et al. (2002) Identification of AHNAK as a novel autoantigen in systemic lupus erythematosus. Biochem. Biophys. Res. Commun. **291:** 951–958
6 Konstantinov K., Mikecz A. von, Buchwald D., Jones J., Gerace L. and Tan E. M. (1996) Autoantibodies to nuclear envelope antigens in chronic fatigue syndrome. J. Clin. Invest. **98:** 1888–1896
7 Ohguro H., Ogawa K., Maeda T., Maeda A. and Maruyama I. (1999) Cancer-associated retinopathy induced by both anti-recoverin and anti-hsc70 antibodies in vivo. Invest. Ophthalmol. Vis. Sci. **40:** 3160–3167
8 Hembrough T. A., Li L. and Gonias S. L. (1996) Cell-surface cytokeratin 8 is the major plasminogen receptor on breast cancer cells and is required for the accelerated activation of cell-associated plasminogen by tissue-type plasminogen activator. J. Biol. Chem. **271:** 25684–25691
9 Hembrough T. A., Vasudevan J., Allietta M. M., Glass W. F. and Gonias S. L. (1995) A cytokeratin 8-like protein with plasminogen-binding activity is present on the external surfaces of hepatocytes, HepG2 cells and breast carcinoma cell lines. J. Cell Sci. **108:** 1071–1082
10 Wells M. J., Hatton M. W., Hewlett B., Podor T. J., Sheffield W. P. and Blajchman M. A. (1997) Cytokeratin 18 is expressed on the hepatocyte plasma membrane surface and interacts with thrombin-antithrombin complexes. J. Biol. Chem. **272:** 28574–28581

11 Balzar M., Winter M. J., Boer C. J. de and Litvinov S. V. (1999) The biology of the 17-1A antigen (Ep-CAM). J. Mol. Med. **77:** 699–712

12 De Jager W., Te Velthuis H., Prakken B. J., Kuis W. and Rijkers G. T. (2003) Simultaneous detection of 15 human cytokines in a single sample of stimulated peripheral blood mononuclear cells. Clin. Diagn. Lab. Immunol. **10:** 133–139

13 Gharib T. G., Chen G., Wang H., Huang C. C., Prescott M. S., Shedden K. et al. (2002) Proteomic analysis of cytokeratin isoforms uncovers association with survival in lung adenocarcinoma. Neoplasia **4:** 440–448

14 Fukunaga Y., Bandoh S., Fujita J., Yang Y., Ueda Y., Hojo S. et al. (2002) Expression of cytokeratin 8 in lung cancer cell lines and measurement of serum cytokeratin 8 in lung cancer patients. Lung Cancer **38:** 31–38

15 Punglia R. S., D'Amico A. V., Catalona W. J., Roehl K. A. and Kuntz K. M. (2003) Effect of verification bias on screening for prostate cancer by measurement of prostate-specific antigen. N. Engl. J. Med. **349:** 335–342

16 Zeller K. I., Jegga A. G., Aronow B. J., O'Donnell K. A. and Dang C. V. (2003) An integrated database of genes responsive to the Myc oncogenic transcription factor: identification of direct genomic targets. Genome Biol. **4:** R69

17. Dang C. V., Resar L. M., Emison E., Kim S., Li Q., Prescott J. E. et al. (1999) Function of the c-Myc oncogenic transcription factor. Exp. Cell Res. **253:** 63–77

18 Boxer L. M. and Dang C. V. (2001) Translocations involving c-myc and c-myc function. Oncogene **20:** 5595–5610

19 Rodrigo J. P., Lazo P. S., Ramos S., Alvarez I. and Suarez C. (1996) MYC amplification in squamous cell carcinomas of the head and neck. Arch. Otolaryngol. Head Neck Surg. **122:** 504–507

20 Pauli C., Munz M., Kieu C., Mack B., Breinl P., Wollenberg B. et al. (2003) Tumor-specific glycosylation of the carcinoma-associated epithelial cell adhesion molecule EpCAM in head and neck carcinomas. Cancer Lett. **193:** 25–32

21 Vaidya M. M., Sawant S. S., Borges A. M., Naresh N. K., Purandare M. C. and Bhisey A. N. (2000) Cytokeratin expression in human fetal tongue and buccal mucosa. J. Biosci. **25:** 235–242

22 Nagase T., Kikuno R. and Ohara O. (2001) Prediction of the coding sequences of unidentified human genes. XXII. The complete sequences of 50 new cDNA clones which code for large proteins. DNA Res. **8:** 319–327

23 Ross C. D., Gomaa M. A., Gillies E., Juengel R. and Medina J. E. (2000) Tumor grade, microvessel density, and activities of malate dehydrogenase, lactate dehydrogenase, and hexokinase in squamous cell carcinoma. Otolaryngol. Head Neck Surg. **122:** 195–200

24 Aso T., Yamazaki K., Amimoto K., Kuroiwa A., Higashi H., Matsuda Y. et al. (2000) Identification and characterization of Elongin A2, a new member of the Elongin family of transcription elongation factors, specifically expressed in the testis. J. Biol. Chem. **275:** 6546–6552

25 Perry S. V. (2001) Vertebrate tropomyosin: distribution, properties and function. J. Muscle Res. Cell Motil. **22:** 5–49

26 Leyva J. A. (2003) Understanding ATP synthesis: structure and mechanism of the F1-ATPase. Mol. Membr. Biol. **20:** 27–33

27 Xue C., Takahashi M., Hasunuma T., Aono H., Yamamoto K., Yoshino S. et al. (1997) Characterisation of fibroblast-like cells in pannus lesions of patients with rheumatoid arthritis sharing properties of fibroblasts and chondrocytes. Ann. Rheum. Dis. **56:** 262–267

28 Bachvaroff R. J., Miller F. and Rapaport F. T. (1980) Appearance of cytoskeletal components on the surface of leukemia cells and of lymphocytes transformed by mitogens and Epstein-Barr virus. Proc. Natl. Acad. Sci. USA **77:** 4979–4983

29 Aubry M., Marineau C., Zhang F. R., Zahed L., Figlewicz D., Delattre O. et al. (1992) Cloning of six new genes with zinc finger motifs mapping to short and long arms of human acrocentric chromosome 22 (p and q11.2). Genomics **13:** 641–648

30 Meza-Zepeda L. A., Forus A., Lygren B., Dahlberg A. B., Godager L. H., South A. P. et al. (2002) Positional cloning identifies a novel cyclophilin as a candidate amplified oncogene in 1q21. Oncogene. **21:** 2261–2269

31 Kobayashi S., Tanaka T., Matsuyoshi N. and Imamura S. (1996) Keratin 9 point mutation in the pedigree of epidermolytic hereditary palmoplantar keratoderma perturbs keratin intermediate filament network formation. FEBS Lett. **386:** 149–155

32 Wang K., Knipfer M., Huang Q. Q., Heerden A. van, Hsu L. C., Gutierrez G. et al. (1996) Human skeletal muscle nebulin sequence encodes a blueprint for thin filament architecture: sequence motifs and affinity profiles of tandem repeats and terminal SH3. J. Biol. Chem. **271:** 4304–4314

33 Long G. L., Chandra T., Woo S. L., Davie E. W. and Kurachi K. (1984) Complete sequence of the cDNA for human alpha 1-antitrypsin and the gene for the S variant. Biochemistry. **23:** 4828–4837

34 Arlaud G. J., Gaboriaud C., Garnier G., Circolo A., Thielens N. M., Budayova-Spano M. et al. (2002) Structure, function and molecular genetics of human and murine C1r. Immunobiology **205:** 365–382